ELSEVIER

www.elsevier.nl/locate/jorganchem

Journal of Organometallic Chemistry 621 (2001) 55–65

Journal of Organometallic Chemistry

Reactions of Cp*Ir(2,5-dimethylthiophene) with electrophiles, acids, and maleic anhydride

Jiabi Chen [1], Robert J. Angelici *

Ames Laboratory and Department of Chemistry, Iowa State University, Ames IA 50011, USA

Received 17 August 2000; accepted 18 September 2000

Dedicated to Professor Henri Brunner on the occasion of his 65th birthday

Abstract

This paper describes reactions of the two isomers (η^5-Cp*)Ir(η^4-2,5-Me_2T) (**1**) and (η^5-Cp*)Ir(C,S-2,5-Me_2T) (**2**), where 2,5-Me_2T is 2,5-dimethylthiophene, with several electrophiles, acids, and maleic anhydride. The reactions of **1** and **2** with methyl iodide give the same product Cp*Ir(η^4-2,5-Me_2T·CH_3)$^+$ in which the CH_3^+ is bonded to the sulfur atom, as established by X-ray studies. The reaction of **1** with maleic anhydride gives two structurally characterized products: Cp*Ir[η^1(S)-Cp*Ir(η^4-2,5-Me_2T)][η^2-$C_4H_2O_3$] (**13**), in which S-coordinated Cp*Ir(η^4-2,5-Me_2T) and η^2-maleic anhydride are ligands to the Cp*Ir unit, and another product (**12**) that has the composition of **13** except for one additional oxygen atom. Complex **12**, with a complicated and unusual structure, is also isolated from the reaction of maleic anhydride and the acylthiolate Cp*Ir[η^4-C_3H_2MeC(=O)Me] (**14**). Reactions of **1** and **2** with a variety of other agents (MeS–SMe_2^+, CF_3SO_3H, HCl, H_2S, EtOH and I_2) are also described.

Keywords: Iridium complexes; Hydrodesulfurization; Maleic anhydride; Thiophene; Pentamethylcyclopentadienyl

1. Introduction

In studies of the coordination and reactions of thiophenes in transition metal complexes, we observed [1–3] that a two-electron reduction of Cp*Ir(η^5-2,5-Me_2T)$^{2+}$ converts the η^5-2,5-di-methylthiophene (2,5-MeT) ligand to a η^4-2,5-Me_2T ligand in Cp*Ir(η^4-2,5-Me_2T) (**1**), which in the presence of bases or light rearranges to the ring-opened Cp*Ir(C,S-2,5-Me_2T) (**2**) isomer Eq. (1).

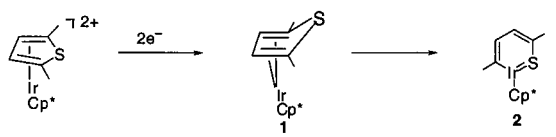

(1)

Although **1** and **2** have been shown to exhibit a range of reactivities [4], there are a few that are particularly relevant to the studies reported in this paper. Lewis acids (A) commonly react with both **1** and **2** to give adducts [4] in which the Lewis acid adds to the strongly donating sulfur atom of **1** Eq. (2). (In its reactions with Lewis acids, isomer **2** rearranges to **1** during adduct formation.)

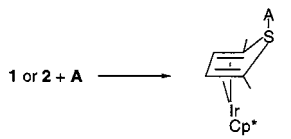

(2)

A = BH_3, CH_3^+, CS_2, $Fe(CO)_4$, $Fe_2(CO)_7$, $Ru(\eta^6$-$C_6H_6)Cl_2$, $Mo_2(CO)_4Cp_2$, $W_2(CO)_4Cp_2$, $Co_4(CO)_{11}$, $Ru_3(CO)_{11}$, $Re_2(CO)_9$, $Fe_2S_2(CO)_5$, $Fe_2(CO)_5(\mu$-$SBu^n)_2$[4]

In this paper are described reactions of **1** and **2** with electrophiles (MeI and MeS–SMe_2^+) and Bronsted acids (CF_3SO_3H, HCl, H_2S, and EtOH) which sometimes give adducts of the type in Eq. (2), but often give other products.

* Corresponding author. Tel.: +1-515-2942603; fax: +1-515-2940105.

E-mail address: angelici@iastate.edu (R.J. Angelici).

[1] Permanent address: Shanghai Institute of Organic Chemistry, Chinese Academy of Sciences, Shanghai, People's Republic of China.

0022-328X/01/$ - see front matter
PII: S0022-328X(00)00752-X

Oxidative addition of H_2 to **1** and **2** yields [5] the dihydride product Cp*Ir(C,S-2,5-Me_2T)$(H)_2$ (Eq. (3)). We find in the present studies that **2** reacts oxidatively with I_2, but a quite different type of product is formed.

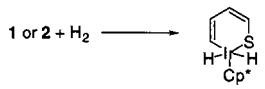

(3)

In earlier investigations [6] of reactions of **1** and **2** with olefins and acetylenes, we observed that there were no reactions between **1** and **2** and 1-hexene, 1,3-cyclohexadiene, 1,3-cyclooctadiene, phenylacetylene, diphenylacetylene, and 3-hexyne. However, the thioether alkynes (MeS–C≡C–Y) did react with **1** and **2** to give bicyclocarbene products of the type shown in Eq. (4). The sulfur atom

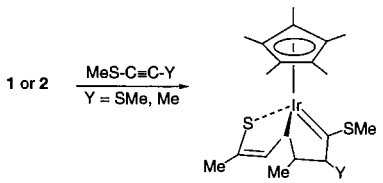

(4)

clearly plays an important role in these reactions. The only other alkyne that reacted with **2** was MeO_2C–C≡C–CO_2Me. While it yielded a pure product with the composition Cp*Ir(2,5-Me_2T)·4MeO_2C–C≡C–CO_2Me, it could not be characterized crystallographically. As the electron-withdrawing ester groups appeared to activate this alkyne for reaction with **1** and **2**, we examined the reactions of **1** and **2** with maleic anhydride, an olefin with an electron-withdrawing anhydride group. Indeed, these reactions lead to some surprising products which are described herein.

2. Experimental

2.1. General procedures

All reactions were carried out using standard Schlenk techniques in an atmosphere of purified nitrogen. All solvents were reagent grade and dried by refluxing over appropriate drying agents and stored over 4 Å molecular sieves under an N_2 atmosphere. Diethyl ether (Et_2O) was distilled from potassium benzophenone ketyl; hexanes and CH_2Cl_2 were distilled from CaH_2. EtOH was distilled from magnesium ethoxide. Maleic anhydride, CF_3SO_3H, CH_3I, and I_2 were purchased from 3M, Fisher Scientific, and Eastman Kodak, respectively. The gases HCl and H_2S were used as purchased. Cp*Ir(η^4-2,5-Me_2T) (**1**) [2,3], Cp*Ir(C,S-2,5-Me_2T) (**2**) [1,2], [Cp*Ir(η^4-2,5-Me_2T·CH_3)](BF_4) [7], and Cp*Ir(η^4-SC_3H_2MeC(=O)Me [8] were prepared as previously reported. Li(NPr^i_2) [9] and (MeS–SMe_2)BF_4 [10] were prepared by literature methods. Elemental analyses were performed by the Galbraith Laboratory or the Shanghai Institute of Organic Chemistry. The ^{1}H-NMR spectra were recorded on a Nicolet NT-300 spectrometer in solutions of $CDCl_3$ with $CHCl_3$ as the internal reference. Electron ionization mass spectra (EIMS) were run on a Finnigan 4000 spectrometer. The fast atom bombardment (FAB) spectra were run on a Kratos MS-50 mass spectrometer using a 3-nitrobenzyl alcohol–CH_2Cl_2 matrix.

2.2. Reaction of Cp*Ir(η^4-2,5-Me_2T) (**1**) with CH_3I to give [Cp*Ir(η^4-2,5-Me_2T·CH_3)]I (**3**)

To a stirred solution of **1** (0.030 g, 0.068 mmol) in CH_2Cl_2 (20 ml) was added 0.50 ml (1.14 g, 8.03 mmol) of CH_3I. The solution was stirred at room temperature (r.t.) for 10 h during which time the light yellow solution gradually turned orange. After vacuum removal of the solvent, the remaining residue was recrystallized from hexane–CH_2Cl_2 at −25°C to give 0.025 g (63%, based on **1**) of white crystalline **3** (m.p. (dec.) 118–120°C). ^{1}H-NMR ($CDCl_3$): δ 5.07 (s, 2H), 2.27 (s, 3H), 2.03 (s, 15H), 1.59 (s, 6H). EIMS: m/e 582 [M^+], 455 [$M^+ - I$], 440 [$M^+ - CH_3I$]. Anal. Calc. for $C_{17}H_{26}$ISIr: C, 35.91; H, 4.51. Found: C, 35.96; H, 4.30%.

2.3. Reaction of Cp*Ir(C,S-2,5-Me_2T) (**2**) with CH_3I to give **3**

A CH_2Cl_2 (15 ml) solution of 0.020 g (0.045 mmol) of **2** was treated, as above for the reaction of **1** with CH_3I, with 0.50 ml (1.14 g, 8.03 mmol) of CH_3I to give 0.014 g (54%, based on **2**) of white crystalline **3** which was characterized by its m.p. and ^{1}H-NMR spectrum.

2.4. Reaction of **3** with Li(NPr^i_2) to give Cp*Ir(C,S-2,5-Me_2TCH_2) (**4**)

To a solution of **3** (0.045 g, 0.077 mmol) in THF (20 ml) was added a fresh Li(NPr^i_2) solution prepared by the reaction of $HNPr^i_2$ (0.009 g, 0.089 mmol) with n-C_4H_9Li (0.048 ml of 2.26 M solution, ~0.089 mmol) in 5 ml of THF at −30°C. The light yellow solution immediately turned green. The mixture was stirred at −30 to 0°C for 4 h during which time the solution gradually turned from green to dark orange. After vacuum removal of the solvent, the residue was chromatographed on Al_2O_3 (neutral) with hexanes–CH_2Cl_2 (5:1) as the eluent. An orange band was eluted and collected. The solvent was removed in vacuo, and the residue was recrystallized from hexanes–CH_2Cl_2 at −80°C to give 0.018 g (51%, based on **3**) of red crystalline **4** (m.p. (dec.) 190–191°C). ^{1}H-NMR ($CDCl_3$): δ 7.69 (dd, 1H), 7.52 (dd, 1H), 6.00 (s, 2H), 2.58 (s, 3H), 1.98

(s, 3H), 1.72 (s, 15H). MS: *m/e* 454 [M^+], 440 [$M^+ - CH_2$]. Anal. Calc. for $C_{17}H_{25}SIr$: C, 45.01; H, 5.55. Found: C, 44.68; H, 5.78%.

2.5. Reaction of [Cp*Ir(η⁴-2,5-Me₂T·CH₃)](BF₄) with Li(NPr$^i_2$) to give 1

A sample of [Cp*Ir(η^4-2,5-Me_2T·CH_3)](BF_4) (0.050 g, 0.095 mmol) was dissolved in 15 ml of THF at −40°C, and a fresh Li(NPr^i_2) solution prepared by the reaction of $HNPr^i_2$ (0.011 g, 0.108 mmol) with *n*-C_4H_9Li (0.06 ml of 2.26 M solution, ~0.109 mmol) in THF (5 ml) was added. The solution immediately turned green. The reaction mixture was stirred at −40 to 0°C for 4 h during which time the green solution gradually turned dark orange. After evaporating the solution under vacuum to dryness, the residue was chromatographed on Al_2O_3 (neutral) with hexanes as the eluent. A light yellow band was eluted and collected. The solvent was removed in vacuo, and the residue was recrystallized from hexanes at −80°C to give 0.019 g (45%) of **1** as light yellow crystals (m.p. (dec.) 117–118°C). ^{1}H-NMR ($CDCl_3$): δ 4.53 (s, 2H), 1.92 (s, 15H), 1.11 (s, 6H).

2.6. Reaction of 1 with (MeS–SMe₂)BF₄ to give [Cp*Ir(η⁴-2,5-Me₂T·SMe)](BF₄) (5)

To a solution of **1** (0.032 g, 0.073 mmol) in 20 ml of CH_2Cl_2 was added (MeS–SMe_2)BF_4 (0.016 g, 0.082 mmol) at −30°C. The light yellow solution quickly turned orange to dark orange. The mixture was stirred at −30 to −20°C for 4 h. After vacuum removal of the solvent, the residue was extracted with hexanes–CH_2Cl_2 (2:1) twice (5 ml × 2). The combined extracts were evaporated under vacuum to dryness, and the residue was recrystallized from hexanes–THF (1:1) at −80°C to give orange–yellow crystals of **5** (m.p. (dec.) 48–50°C). Yield: 0.025 g (64%, based on **1**). ^{1}H-NMR ($CDCl_3$): δ 5.28 (s, 2H), 2.39 (s, 6H), 2.31 (s, 3H), 2.02 (s, 15H). MS: *m/e* 487 [$M^+ - BF_4$]. Anal. Calc. for $C_{17}H_{26}S_2IrBF_4$: C, 35.60; H, 4.57. Found: C, 35.69; H, 4.25%.

2.7. Reaction of 2 with (MeS–SMe₂)BF₄ to give [Cp*Ir(C,S-2,5-Me₂T)SMe](BF₄) (6)

Similar to the procedure described in the reaction of **1** with (MeS–SMe_2)BF_4, 0.050 g (0.114 mmol) of **2** in CH_2Cl_2 (25 ml) was treated with (MeS–SMe_2)BF_4 (0.023 g, 0.117 mmol) at −30 to 0°C for 4 h during which time the red solution gradually turned orange. After vacuum removal of the solvent, the residue was extracted with hexanes–CH_2Cl_2 (2:1) twice (10 ml × 2). The combined extracts were evaporated under vacuum to dryness, and the residue was recrystallized from hexanes–THF at −80°C to give 0.042 g (68%, based on **2**) of orange crystalline **6** (m.p. (dec.) 234–236°C). ^{1}H-NMR ($CDCl_3$): δ 5.82 (d, 1H), 5.54 (d, 1H), 2.52 (s, 3H), 2.07 (s, 3H), 1.97 (s, 15H), 1.94 (s, 3H). MS: *m/e* 487 [$M^+ - BF_4$]. Anal. Calc. for $C_{17}H_{26}S_2IrBF_4$: C, 35.60; H, 4.57. Found: C, 35.90; H, 4.25%.

2.8. Reaction of 1 with CF₃SO₃H to give [Cp*Ir(2,5-Me₂T·H](CF₃SO₃) (7)

To a stirred solution of **1** (0.035 g, 0.080 mmol) in CH_2Cl_2 (5 ml) was added 0.012 g (0.080 mmol) of CF_3SO_3H by syringe. The light yellow solution immediately turned orange. After stirring for 10 min at r.t., the solvent was evaporated in vacuo to dryness. The orange residue was recrystallized from Et_2O–CH_2Cl_2 at −80°C to give 0.038 g (81%, based on **1**) of orange–yellow powder **7**. ^{1}H-NMR ($CDCl_3$): δ 5.82 (d, 1H), 4.67 (m, 1H), 4.22 (d, 1H), 2.57 (s, 3H), 2.06 (s, 15H), 0.83 (d, 3H). MS (FAB): *m/e* 441 [M^+]. Anal. Calc. for $C_{17}H_{24}O_3F_3S_2Ir$: C, 34.62; H, 4.10. Found: C, 34.38; H, 4.28%.

2.9. Reaction of 2 with CF₃SO₃H to give 7

To a solution of **2** (0.035 g, 0.080 mmol) in CH_2Cl_2 (5 ml) was added 0.012 g (0.080 mmol) of CF_3SO_3H by syringe. The red solution immediately turned orange. After 10 min stirring at r.t., the solvent was evaporated to dryness in vacuo. Further treatment of the remaining residue as described above for the reaction of **1** with CF_3SO_3H gave 0.036 g (76%, based on **2**) of **7** as an orange–yellow powder which was identified by its ^{1}H-NMR and mass spectra.

2.10. Reaction of 1 with HCl (gas) to give Cp*Ir(η⁴-2,5-Me₂T·H)Cl (8)

Into a CH_2Cl_2 (30 ml) solution of **1** (0.030 g, 0.068 mmol) at −40°C was bubbled HCl gas. The light yellow solution immediately turned purple–red. After bubbling for 1 min at −40 to −35°C, the solvent was evaporated to dryness under vacuum, and the remaining residue was recrystallized from hexanes–CH_2Cl_2 solution at −80°C to give 0.018 g (56%, based on **1**) of light yellow crystalline **8** (m.p. (dec.) 96°C). ^{1}H-NMR ($CDCl_3$): δ 5.27 (s, 2H), 2.38 (s, 1H), 2.10 (s, 6H), 1.58 (s, 15H). EIMS: *m/e* 476 [M^+], 441 [$M^+ - Cl$], 440 [$M^+ - HCl$]. Anal. Calc. for $C_{16}H_{24}ClSIr{\cdot}2CH_2Cl_2$: C, 33.47; H, 4.37. Found: C, 33.77; H, 4.41%.

2.11. Reaction of 2 with HCl (gas) to give 8

As described above for the reaction of **1** with HCl gas, **2** (0.022 g, 0.050 mmol) in 30 ml of CH_2Cl_2 at −40°C was treated with HCl. The red solution imme-

diately turned yellow. After 1 min, the resulting solution was treated as above to give 0.013 g (54%, based on **2**) of light yellow crystalline **8** which was identified by its m.p. and ^{1}H-NMR spectrum.

2.12. Reaction of **1** with H_2S to give $Cp^*Ir(2,5\text{-}Me_2T)(H_2S)$ (**9**)

Into a solution of 0.030 g (0.068 mmol) of **1** dissolved in 30 ml of CH_2Cl_2 was bubbled H_2S gas at 15–20°C for 3 h during which time the light yellow solution turned golden yellow to brown–yellow. After vacuum removal of the solvent, the remaining residue was recrystallized from hexanes–CH_2Cl_2 at −80°C to give 0.012 g (37%, based on **1**) of orange crystalline **9** (m.p. (dec.) 123–124°C). ^{1}H-NMR ($CDCl_3$): δ 7.69 (d, 1H), 7.51 (d, 1H), 4.20 (m, 2H), 1.68 (s, 3H), 1.30 (s, 15H), 0.90 (t, 3H). EIMS: m/e 474 [M^+], 472 [$M^+ - 2H$], 392 [$Cp^*IrS_2^+$]. Anal. Calc. for $C_{16}H_{25}S_2Ir$: C, 40.57; H, 5.32. Found: C, 41.00; H, 5.13%.

2.13. Reaction of **2** with H_2S to give **9**

As for the preceding synthesis, H_2S gas was bubbled into a solution of **2** (0.030 g, 0.068 mmol) in 30 ml of CH_2Cl_2 at 15–20°C for 3 h. The color of the solution changed from red to brown–yellow. Subsequent treatment of the resulting solution as described for the reaction of **1** with H_2S gave 0.014 g (44%, based on **2**) of **9** as orange crystals which were identified by their m.p. and ^{1}H-NMR spectrum.

2.14. Reaction of **1** with EtOH to give $Cp^*Ir(2,5\text{-}Me_2T)(EtOH)$ (**10**)

To a stirred solution of **1** (0.035 g, 0.080 mmol) in CH_2Cl_2 (20 ml) at r.t. was added 0.5 ml (0.393 g, 8.52 mmol) of EtOH (absolute). The solution was stirred at r.t. for 6 h during which time the light yellow solution gradually turned orange. After evaporation of the solvent to dryness in vacuo, the remaining residue was recrystallized from hexanes–CH_2Cl_2 solution at −80°C to give orange–yellow crystals of **10**, yield 0.012 g (31%, based on **1**) (m.p. (dec.) 103–105°C). ^{1}H-NMR ($CDCl_3$): δ 6.20 (d, 1H), 6.08 (m, 1H), 5.68 (d, 1H), 3.71 (q, 2H), 1.96 (s, 3H), 1.86 (s, 3H), 1.62 (s, 15H), 1.22 (t, 3H). EIMS: m/e 486 [M^+], 441 [$M^+ -$ OEt], 440 [$M^+ -$ EtOH]. Anal. Calc. for $C_{18}H_{29}OSIr$: C, 44.51; H, 6.02. Found: C, 44.88; H, 6.48%.

2.15. Reaction of **2** with I_2 to give $(Cp^*IrI_2)_2$ (**11**)

To a solution of **2** (0.020 g, 0.045 mmol) in 20 ml of THF (or acetone) was added 0.012 g (0.095 mmol) of I_2 at −30°C. The mixture was stirred at −30°C to 0°C for 4 h during which time the purple solution turned dark red. After evaporating the solution in vacuo to dryness, the dark red residue was dissolved in CH_2Cl_2. The solution was filtered to remove insoluble materials. The filtrate was evaporated and the residue was recrystallized from hexanes–CH_2Cl_2 solution at −80°C to give black–red crystals of **11**, yield 0.021 g (81%, based on **2**) (m.p. (dec.) 280°C). ^{1}H-NMR ($CDCl_3$): δ 1.89 (s, Cp*). MS: m/e 1036 [$M^+ -$ I], 909 [$M^+ - 2$I]. Anal. Calc. for $C_{20}H_{30}I_4Ir_2$: C, 20.66; H, 2.60. Found: C, 20.82; H, 2.65%.

2.16. Reaction of **1** with maleic anhydride to give $Cp^*Ir[SC_3H_2MeC(=O)Me\cdot C_4H_2O_3]$ (**12**) and $Cp^*Ir[\eta^1(S)\text{-}Cp^*Ir(\eta^4\text{-}2,5\text{-}Me_2T)](\eta^2\text{-}C_4H_2O_3))$ (**13**)

A sample of **1** (0.040 g, 0.091 mmol) was dissolved in 30 ml of THF at r.t. To this solution was added 0.018 g (0.18 mmol) of maleic anhydride. The mixture was stirred at r.t. for 30 h. The resulting orange solution was evaporated under vacuum to dryness, and the residue was chromatographed on SiO_2 with hexane–CH_2Cl_2–Et_2O (1:1:0.5) as the eluent. A yellow band eluted first; then an orange band was eluted with CH_2Cl_2–Et_2O (1:1). The solvents were removed from the above eluates, and the residues were recrystallized from hexanes–CH_2Cl_2 solution at −80°C. From the first fraction, 0.010 g (20%, based on **1**) of orange crystalline **12** was obtained (m.p. (dec.) 141–142°C). ^{1}H-NMR ($CDCl_3$): δ 3.95 (d, 1H), 3.64 (d, 1H), 3.50 (d, 1H), 3.02 (d, 1H), 2.10 (s, 3H), 1.94 (s, 3H), 1.80 (s, 15H). MS: m/e 554 [M^+]. Anal. Calc. for $C_{20}H_{25}O_4SIr$: C, 43.78; H, 4.55. Found: C, 43.29; H, 4.72%. From the second fraction, 0.012 g (15%, based on **1**) of **13** as orange–yellow crystals was obtained (m.p. (dec.) 165–167°C). ^{1}H-NMR ($CDCl_3$): δ 4.19 (s, 2H), 3.13 (s, 2H), 1.92 (s, 15H), 1.61 (s, 15H), 0.99 (s, 6H). MS: m/e 866 [M^+], 768 [$M^+ - C_4H_2O_3$]. Anal. Calc. for $C_{30}H_{40}O_3SIr_2$: C, 41.65; H, 4.66. Found: C, 41.22; H, 5.01%.

2.17. Reaction of **2** with maleic anhydride to give **12**

As described above for the reaction of **1** with maleic anhydride, **2** (0.030 g, 0.068 mmol) was reacted with 0.014 g (0.14 mmol) of maleic anhydride in THF (30 ml) at −40 to −20°C for 24 h. Subsequent treatment of the resulting mixture as described for the reaction of **1** with maleic anhydride yielded 0.016 g (42%, based on **2**) of orange crystalline **12**, which was identified by its melting point, ^{1}H-NMR and MS spectra.

2.18. Reaction of $Cp^*Ir(\eta^4\text{-}SC_3H_2MeC(=O)Me$ (**14**) with maleic anhydride to give **12**

To a solution of $Cp^*Ir(\eta^4\text{-}SC_3H_2MeC(=O)Me)$ (0.015 g, 0.022 mmol) in 20 ml of THF at −40°C was added

0.006 g (0.061 mmol) of maleic anhydride. The reaction mixture was stirred at −40 to 20°C for 24 h during which time the light yellow solution gradually turned orange. Further treatment of the resulting solution in a manner similar to that described above for the reaction of **1** with maleic anhydride gave 0.009 g (75%) of **12** as orange crystals which were identified by their melting point and ^{1}H-NMR spectra.

2.19. X-ray crystal structure determinations of 3, 12 and 13

Crystals of complexes **3**, **12** and **13** suitable for X-ray diffraction studies were obtained by recrystallization from hexanes–CH_2Cl_2 solution. The single crystals were mounted on the end of a glass fiber. The X-ray diffraction intensity data were collected by using Enraf–Nonius CAD4, Siemens P4RA, and Rigaku AFC7R diffractometers, respectively. The cell constants were determined from a list of reflections found by an automated search routine.

For **3**, the systematic absences unambiguously indicated that the space group was *Pbcn* (no. 60). The Ir, S, and I atoms were placed based on a direct method E-map [11]. The remaining non-hydrogen atoms were located in a subsequent difference Fourier map. In the final stages of the refinement, all 20 non-hydrogen atoms were given anisotropic temperature factors, and secondary extinction coefficients were included (refining to a value of $8(1) \times 10^{-9}$, in absolute units). Hydrogen atoms were not considered in the model. The final refinement cycles involved 182 parameters which were fit to 1784 observed data.

For complex **12**, the space group was chosen based on systematic absences and intensity statistics. This assumption proved to be correct based on a successful direct methods solution [12] and subsequent refinement of the structure. All non-hydrogen atoms were placed directly from the E-map and refined with anisotropic thermal parameters. Hydrogen atoms were refined in one of two ways: (1) methyl hydrogens were refined as idealized groups with common isotropic displacement parameters or (2) tertiary hydrogens were refined as isotropic atoms with joint isotropic displacement parameters.

The structure of complex **13** was solved by heavy-atom Patterson methods and expanded using Fourier techniques. Some non-hydrogen atoms were refined anisotropically, while the rest were refined isotropically. Hydrogen atoms were included but not refined. The final cycle of the full-matrix least-squares refinement was based on 2345 observed reflections ($I > 3.0\sigma(I)$) and 242 variable parameters.

All the calculations were performed using the CAD4-SDP, SHELXTL-Plus programs, or the TEXSAN crystallographic software package of the Molecular Structure Corporation. Details of the crystallographic data and procedures used in the data collection and reduction for complexes **3**, **12**, and **13** are given in Table 1. Selected bond lengths and angles are listed in Table 2. The molecular structures for **3**, **12**, and **13** are given in Figs. 1–3, respectively. The atomic coordinates and B_{iso}/B_{eq}, anisotropic displacement parameters, complete bond lengths and angles, least-squares planes for **3**, **12**, and **13** are given in the Supplementary Material.

3. Results and discussion

3.1. Reactions of 1 and 2 with the electrophiles (MeI and MeS–SMe$_2^+$)

Both **1** and **2** react (Eq. (5)) with MeI at room temperature to give **3** in 63% and 54% yields,

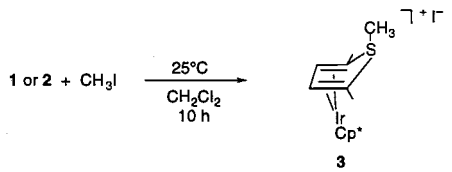

(5)

respectively. These reactions are similar to those (Eq. (2)) of **1** and **2** with other Lewis acids/electrophiles, including the reaction [7] with $Me_3O^+BF_4^-$ to give [Cp*Ir(η^4-2,5-Me_2T·CH_3)]BF_4, which contains the same cation as in **3**, but could not be obtained as X-ray quality crystals. The ^{1}H-NMR spectra of these cations are similar but not identical. In the I^- salt, the 2,5-methyl groups and 3,4-hydrogens are at δ1.59 and 5.07 ppm respectively, whereas the same protons in the BF_4^- salt are at δ1.53 and 4.92 ppm. The S–CH_3 signals are at δ2.27 and 2.08 ppm for the I^- and BF_4^- salts, respectively. As spectra of both salts were measured in $CDCl_3$ solvent, differences in their chemical shifts are presumably due to ion-pairing effects of the different anions.

The structure (Fig. 1) of **3** is very similar to that [1] of the analogous BH_3 adduct Cp*Ir(η^4-2,5-Me_2T·BH_3). The C(2)–S and C(5)–S bonds are similar in both (1.79(2), 1.78(1) Å in **3** and 1.80(1), 1.81(1) in the BH_3 adduct) as well as in Cp*Ir(η^4-2-MeT·BH_3) (1.79(1), 1.79(1)) [7]. In all of these compounds, the C–S bonds are lengthened compared to those in free thiophene (1.72 Å) [13] and in **1** (1.76(2), 1.79(1) Å) [2], although the errors in **1** are relatively large. In **3**, all of the thiophene C–C distances (1.45(2), 1.45(2), 1.46(2)) are the same within experimental error as was also observed for Cp*Ir(η^4-2,5-Me_2T·BH_3) [1], which suggests delocalization in the diene part of the ligand. As expected, the S–CH_3 bond is shorter in **3** (1.83(1) Å) than the S–BH_3 bond (1.97(1)Å) in the BH_3 adduct because the atomic radius of C is smaller than that of B.

The reaction (Eq. (6)) of **3** with lithium diisopropylamide (LDA) gives a red product (**4**) (51% yield) with a composition Cp*Ir(2,5-Me_2TCH_2) that is supported by a parent ion in the mass spectrum

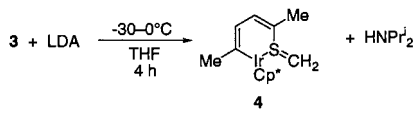

4 (6)

and a satisfactory elemental analysis. The compound is soluble in both polar and non-polar organic solvents and is air-sensitive in solution and the solid state. In the absence of X-ray quality crystals, a proposed structure for **4** must be based on the ^{1}H-NMR spectrum which shows CH_3 signals at δ 2.58s and 1.98s ppm, C–H signals at 7.52dd and 7.69dd, and a CH_2 signal at 6.00s. While the structure proposed for **4** in Eq. (6) accounts for non-equivalent CH_3 and C–H groups as well as a CH_2 unit, it does not explain the doublet-of-doublets splitting of the C–H groups; these signals would be expected to be simple doublets. A structure in which the CH_2 is present as a carbene ligand (Ir=CH_2) seems unlikely as the ^{1}H signal for the CH_2 group occurs at approximately 16 ppm in known Ir=CH_2 compounds [14]. The structure of **4** proposed in Eq. (6) must be regarded as tentative. Rather surprisingly, the reaction of [Cp*Ir(η^4-2,5-Me_2T·CH_3)](BF_4) with LDA does not give **4** but instead the demethylated product **1** in 45% yield. It is not clear why the I^- and BF_4^- anions cause these reactions to give different products.

The reaction (Eq. (7)) of **1** with the electrophilic (MeS–SMe_2)BF_4 gave **5** with a composition

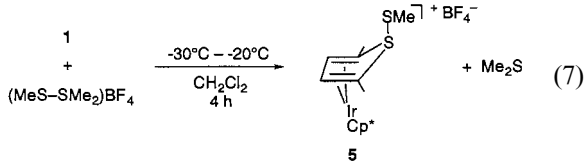

5 (7)

[Cp*Ir(2,5-Me_2T·SMe)]BF_4 that is supported by its mass spectrum and elemental analysis. This air-sensitive complex has a simple ^{1}H-NMR spectrum that shows equivalent 2,5-methyl groups (δ 2.39s ppm), equivalent 3,4-hydrogens (5.28s ppm) and a SMe group (2.31s ppm). These chemical shifts and the lack of hyperfine coupling are consistent with the structure in Eq. (7) that has an SMe^+ group on the thiophene sulfur. The signals for all of these methyl groups are somewhat downfield of those in the related methyl complex **3**.

Table 1
Crystal data and and collection parameters for complexes **3**, **12**, and **13**

	3	**12**	**13**
Formula	$C_{17}H_{26}ISIr$	$C_{20}H_{25}O_4SIr$	$C_{30}H_{40}O_3SIr_2$
Formula weight	581.56	553.7	865.14
Space group	*Pbcn*	$P2_1/c$ (no.14)	$P2_1/c$ (no.14)
a (Å)	22.393(2)	9.376(2)	10.095(4)
b (Å)	12.899(1)	18.082(5)	16.290(4)
c (Å)	13.098	11.675(2)	18.394(5)
β (deg)		106.35(2)	99.01(3)
V (Å^3)	3783.2(8)	1899.4(6)	2987(1)
Z	8	4	4
D_{calc} (g cm^{-3})	2.042	1.936	1.923
Crystal size (mm)	$0.24\times0.10\times0.09$	$0.26\times0.22\times0.05$	$0.20\times0.20\times0.30$
Frequency (Mo–K_α) (cm^{-1})	87.445	14.826 (mm^{-1}, Cu–K_α)	90.22
Radiation (monochromated in incident beam) (Å)	0.71073 (Mo–K_α)	1.54178 (Cu–K_α)	0.71069 (Mo–K_α)
Diffractometer	Enraf-Nonius CAD4	Siemens P4RA	Rigaku AFC7R
Temperature (°C)	−25(1)	−60(1)	20.0
Orientation reflections: no.; range (2θ) (°)	25; $21.1<2\theta<32.0$		22; 18.4–21.7
Scan method	θ–2θ	2θ–θ	ω–2θ
Data collection range, 2θ (°)	4–50.0	4–115.0	5–46.1
Number of unique data, total	3326	2558	4304
with $I>3.00\sigma(I)$	1784	2387 ($F\geq4.0\sigma(F)$)	2345
Number of parameters refined	182	277	242
Correction factors (max., min.)	0.9321, 0.9995	0.0219, 1.0000	0.9128, 1.0000
R [a]	0.0285	0.0319	0.052
Rw [b]	0.0342	0.0400	0.056
Quality-of-fit indicator [c]	0.926	1.49	1.94
Largest shift/esd. Final cycle	0.01	0.020	0.01
Largest peak, (e Å^{-3})	0.6(1)	1.06	1.63
Minimum peak, (e Å^{-3})		−1.54	−1.14

[a] $R=\Sigma||F_o|-|F_c||/\Sigma|F_o|$.
[b] $R_w=[\Sigma w(|F_o|-|F_c|)^2/\Sigma w|F_o|^2]^{1/2}$; $w=1/\sigma^2(|F_o|)$.
[c] Quality of "fit" $=[\Sigma w(|F_o|-|F_c|)^2/(N_{obs}-N_{parameters})]^{1/2}$.

Table 2
Selected bond lengths (Å) [a] and angles (°) [a] for complexes **3**, **12**, and **13**

Complex **3**			
Bond lengths			
Ir–C(2)	2.11(1)	S–C(7)	1.83(1)
Ir–C(3)	2.14(1)	C(1)–C(2)	1.52(1)
Ir–C(4)	2.15(1)	C(2)–C(3)	1.45(2)
Ir–C(5)	2.15(1)	C(3)–C(4)	1.45(2)
S–C(2)	1.79(1)	C(4)–C(5)	1.46(2)
S–C(5)	1.78(1)	C(5)–C(6)	1.50(2)
Bond angles			
C(2)–S–C(5)	85.7(5)	C(2)–C(3)–C(4)	108(1)
S–C(2)–C(3)	109.6(9)	C(3)–C(4)–C(5)	110.6(9)
S–C(2)–C(1)	119(1)	C(4)–C(5)–C(6)	126(1)
S–C(5)–C(4)	108.1(7)	C(2)–S–C(7)	106.5(6)
S–C(5)–C(6)	119.6(9)	C(5)–S–C(7)	108.6(5)
Complex **12**			
Bond lengths			
Ir–S	2.353(1)	C(6)–C(1)	1.527(9)
Ir–C(1)	2.203(8)	C(6)–C(7)	1.529(8)
Ir–C(8)	2.160(6)	C(7)–C(8)	1.526(8)
C(1)–C(2)	1.404(9)	C(7)–C(9)	1.512(9)
C(2)–O(1)	1.332(7)	C(8)–C(10)	1.472(10)
O(1)–C(4)	1.479(7)	C(9)–O(2)	1.185(7)
C(4)–C(5)	1.494(8)	C(9)–O(3)	1.375(8)
C(4)–C(6)	1.551(9)	C(10)–O(3)	1.405(8)
S–C(4)	1.808(7)	C(10)–O(4)	1.205(8)
Bond angles			
S–Ir–C(1)	84.7(2)	C(1)–C(6)–C(7)	107.5(5)
S–Ir–C(8)	86.1(2)	C(6)–C(7)–C(8)	111.3(5)
C(1)–Ir–C(8)	73.2(3)	C(7)–C(8)–C(10)	103.6(5)
Ir–S–C(4)	95.4(2)	Ir–C(8)–C(7)	109.8(4)
Ir–C(1)–C(2)	94.6(5)	Ir–C(8)–C(10)	115.7(5)
Ir–C(1)–C(6)	102.8(5)	C(8)–C(7)–C(9)	104.0(6)
C(2)–C(1)–C(6)	103.3(5)	C(7)–C(9)–O(2)	130.1(7)
C(1)–C(6)–C(4)	99.8(5)	C(7)–C(9)–O(3)	108.8(5)
O(1)–C(4)–C(6)	101.1(5)	C(9)–O(3)–C(10)	110.3(5)
C(2)–O(1)–C(4)	106.6(4)	C(8)–C(10)–O(3)	110.0(5)
C(1)–C(2)–C(3)	130.3(6)	C(1)–C(2)–O(1)	114.3(5)
C(3)–C(2)–O(1)	114.4(5)	O(2)–C(9)–O(3)	120.7(6)
S–C(4)–C(6)	108.5(4)	O(3)–C(10)–O(4)	117.2(7)
O(1)–C(4)–C(5)	107.4(4)	C(8)–C(10)–O(4)	132.7(6)
S–C(4)–C(5)	114.9(5)		
Complex **13**			
Bond lengths			
Ir(1)–C(2)	2.07(2)	Ir(2)–S(1)	2.262(6)
Ir(1)–C(3)	2.08(3)	Ir(2)–C(8)	2.05(3)
Ir(1)–C(4)	2.07(3)	Ir(2)–C(9)	2.08(3)
Ir(1)–C(5)	2.11(3)	C(7)–C(8)	1.49(4)
S(1)–C(2)	1.78(3)	C(8)–C(9)	1.44(4)
S(1)–C(5)	1.77(3)	C(9)–C(10)	1.49(4)
C(2)–C(3)	1.42(4)	O(1)–C(7)	1.40(4)
C(3)–C(4)	1.34(4)	O(1)–C(10)	1.46(5)
C(4)–C(5)	1.41(4)	O(3)–C(7)	1.22(5)
C(1)–C(2)	1.59(4)	O(2)–C(10)	1.17(5)
C(5)–C(6)	1.50(4)		
Bond angles			
C(2)–S(1)–C(5)	79(1)	Ir(2)–C(9)–C(10)	114(2)
S(1)–C(2)–C(3)	114(2)	Ir(2)–C(8)–C(7)	111(2)
C(2)–C(3)–C(4)	105(2)	C(7)–C(8)–C(9)	101(2)
C(3)–C(4)–C(5)	113(2)	C(8)–C(9)–C(10)	115(2)
C(4)–C(5)–S(1)	109(1)	O(1)–C(10)–C(9)	99(2)
Ir(2)–S(1)–C(5)	121.6(10)	O(1)–C(10)–O(2)	120(3)
Ir(2)–S(1)–C(2)	120.8(8)	O(1)–C(7)–C(8)	109(2)
S(1)–Ir(2)–C(8)	90.8(8)	C(7)–O(1)–C(10)	113(2)
S(1)–Ir(2)–C(9)	91.6(8)	O(1)–C(7)–O(3)	122(3)
C(8)–Ir(2)–C(9)	40(1)	O(3)–C(7)–C(8)	127(3)
Ir(2)–C(8)–C(9)	71(1)	O(2)–C(10)–C(9)	139(3)
Ir(2)–C(9)–C(8)	68(1)		

[a] Estimated standard deviations in the least significant figure are given in parentheses.

In contrast to most reactions of **1** and **2**, the reaction (Eq. (8)) of **2** with $MeS–SMe_2^+$ gives a

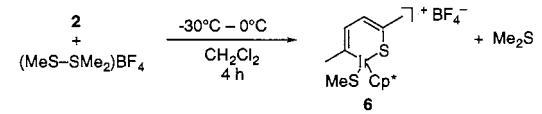

6 (8)

different product than the reaction of **1**. The air-sensitive product **6** has the same composition as **5**, but its ^{1}H-NMR spectrum clearly shows non-equivalent 2,5-methyl groups (δ 2.52s, 2.07s ppm), non-equivalent, coupled C–H groups (5.82d, 5.54d ppm) and an SMe group at δ 1.94s ppm. All of the NMR features are consistent with the thiophene ring-opened structure of the type shown in Eq. (8). The SMe^+ group is shown co-ordinated to Ir, but the experimental evidence does not exclude a structure with the SMe^+ group on the sulfur of the ring-opened thiophene.

3.2. Reactions of *1* and *2* with Bronsted acids

Both **1** and **2** react (Eq. (9)) immediately with CF_3SO_3H to give the same product

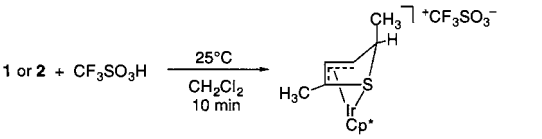

7 (9)

[Cp*Ir(2,5-Me_2T·H)]CF_3SO_3 (**7**) in 81% and 76% yields, respectively. Although X-ray quality crystals could not be obtained, the ^{1}H-NMR spectrum of **7** shows that a proton has added to the 2,5-Me_2T ligand, as was observed by Rauchfuss and co-workers [15] in the reaction of another η^4-2,5-Me_2T complex (η^6-C_6Me_6)Ru(η^4-2,5-Me_2T) with the proton donor NH_4^+. The ^{1}H-NMR spectrum of their product [(η^6-C_6Me_6)Ru(η^r-2,5-Me_2T·H)]$^+$, whose structure (**A**) was established by X-ray diffraction studies, is very similar to that of **7**. The ^{1}H-NMR spectrum of **7** exhibits a

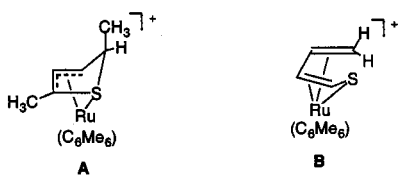

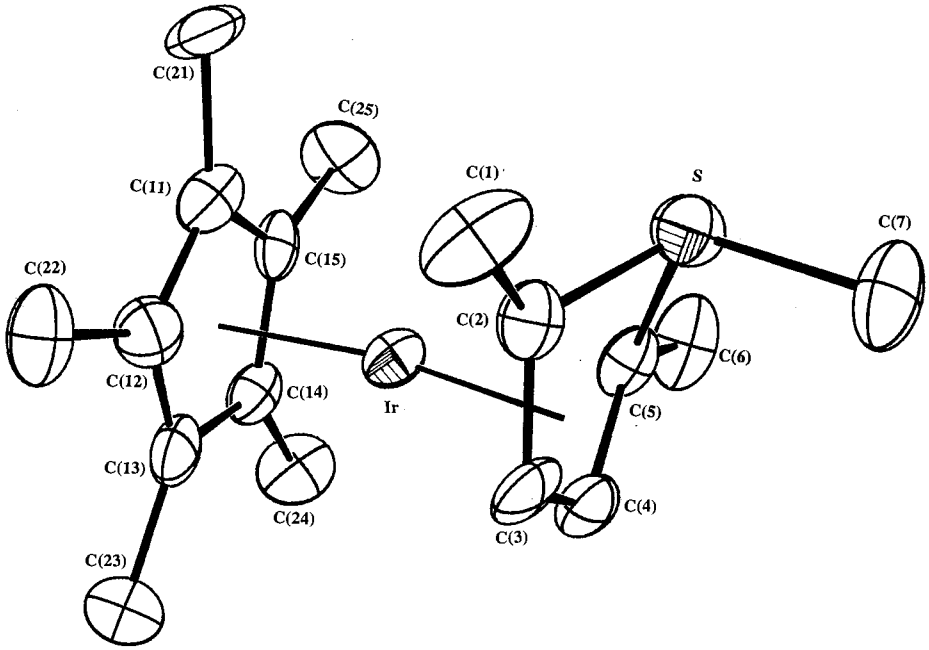

Fig. 1. Thermal ellipsoid drawing of **3**, showing the atom-numbering scheme.

doublet methyl signal at high field (δ 0.83d ppm) for the methyl on the saturated carbon, while the other methyl is a singlet at lower field (2.57s ppm). The hydrogen on the saturated carbon is a multiplet due to coupling with the methyl group and adjacent C–H group. Both of the C–H groups give doublets at δ 5.82 and 4.22 ppm; the C–H adjacent to the saturated carbon would be expected to be a doublet-of-doublets, but one of these coupling constants may be too small to observe. Rauchfuss et al. [16] also reported the slow C–S cleavage of the thiophene analog of **A** [(η^6-C_6Me_6)Ru(η^4-T·H)]$^+$ to give the dienethiolate isomer **B**. Although **A** did not undergo a similar cleavage, it is not possible to exclude the dienethiolate structure for complex **7**. Dienethiolate structures have also been observed [17,18] in a series of (η^5-Cp)Ru(η^5-thiophene·H)$^+$ complexes.

When gaseous HCl, rather than CF_3SO_3H, is reacted with **1** or **2**, yellow **8** is formed. Its Cp*Ir(2,5-Me_2T·H)Cl composition is established by elemental analyses and the parent ion in the mass spectrum. Although one would expect the same product to form with either CF_3SO_3H or HCl, the simplicity of the ^{1}H-NMR spectrum for **8** clearly indicates that it has a much different structure than **7**. The proposed structure in Eq. (10) is consistent with the observed singlet at

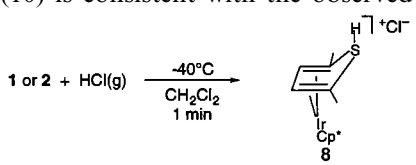

(10)

δ 2.10s ppm for the equivalent methyl groups and the singlet at 5.27s ppm for the 3,4-hydrogens. These absorptions are somewhat downfield of the corresponding signals (δ 1.59s, 5.07 ppm) for the analogous methyl complex Cp*Ir(η^4-2,5-Me_2T·CH_3)$^+$ I^- (**3**). These resonances for **8** are also very similar to those (δ 2.39s, 5.28s ppm) for [Cp*Ir(η^4-2,5-Me_2T·SMe)]BF_4 (**5**). The S–H hydrogen in **8** at δ 2.38s ppm is in the region characteristic of thiols (RSH). While CF_3SO_3H and HCl give different products in their reactions with **1** and **2**, it is not clear why their structures are different unless there are specific interactions between the cationic complexes and their anions (such as hydrogen-bonding between the SH proton and the Cl^-) that stabilize the different structures.

Like CF_3SO_3H and HCl, gaseous H_2S reacts with **1** and **2** to give a product (**9**, in 37% and 44% yields) in which one molecule of H_2S has added to the starting complex. This composition Cp*Ir(2,5-Me_2T)(H_2S) is

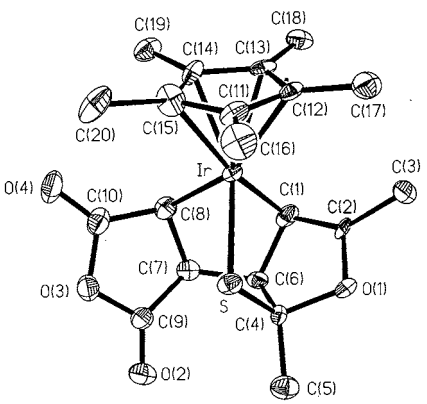

Fig. 2. Thermal ellipsoid drawing of **12**, showing the atom-numbering scheme. Hydrogen atoms not shown.

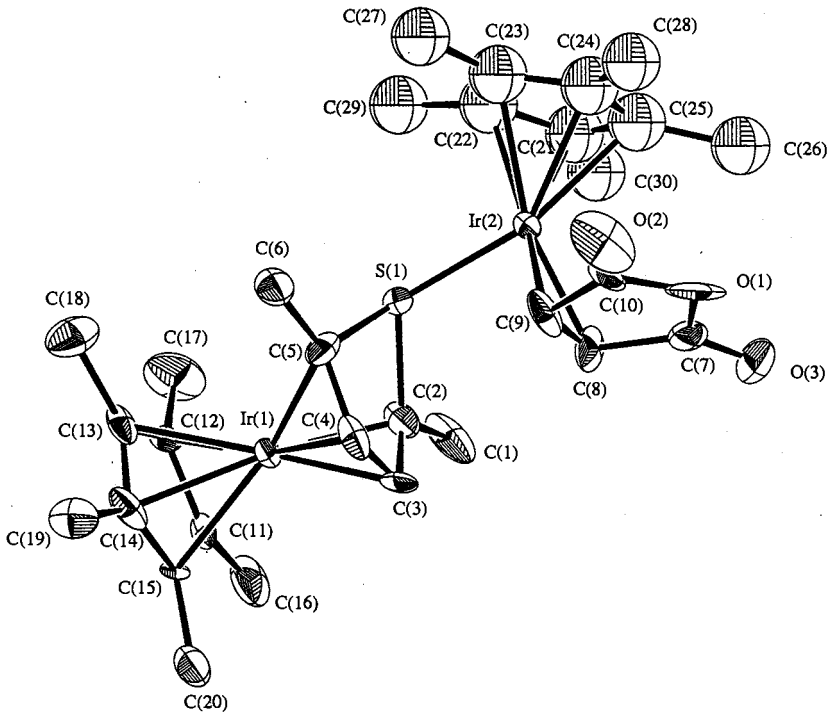

Fig. 3. Thermal ellipsoid drawing of **13**, showing the atom-numbering scheme. Hydrogen atoms not shown.

supported by elemental analyses and a parent ion in the mass spectrum. The ^{1}H-NMR spectrum of **9**, however, shows that its structure is very different from those of either **7** or **8** obtained from the reactions with CF_3SO_3H and HCl. In the ^{1}H-NMR spectrum of **9**, one methyl group gives rise to a singlet (δ 1.68 ppm) while the other (δ 0.9 ppm) is a triplet, which suggests the presence of an ethyl group. Since it was not possible to obtain X-ray quality crystals of **9**, further speculation about its structure is not merited.

Although ethanol is a much weaker acid than the others discussed above, it reacts with **1** to give **10** with the composition Cp*Ir(2,5-Me_2T)(EtOH), which is established by elemental analysis and the parent ion in its mass spectrum. The ^{1}H-NMR spectrum shows non-equivalent methyl groups, non-equivalent 3,4-hydrogens and a CH_3CH_2O group. Our inability to grow X-ray quality crystals does not permit a definitive structural assignment to be made to **10**.

3.3. Reaction of *2* with an oxidizing agent (I_2)

We previously observed (Eq. (3)) that **2** undergoes an oxidative-addition reaction with H_2 to give the dihydride complex Cp*Ir(C,S-2,5-Me_2T)$(H)_2$. Surprisingly, the reaction of **2** with I_2 does not give the analogous diiodide product. Instead, the 2,5-Me_2T ligand was substituted and $(Cp^*IrI_2)_2$ (**11**) was isolated in 81% yield (Eq. (11)). Compound **11**, which was characterized by

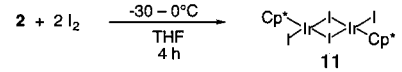

(11)

its elemental analyses, mass spectrum, and ^{1}H-NMR spectrum, was previously reported [19]. The mechanism for reaction (11) presumably involves initial I_2 oxidation of **2** to Cp*Ir(η^5-2,5-MeT)$^{2+}(I^-)_2$. This step is related to the previously reported [1] oxidation of **2** to Cp*Ir(η^5-2,5-Me_2T)$^{2+}$ by $2Cp_2Fe^+$; this reaction is accompanied by ring-closure to form an η^5-2,5-Me_2T ligand. Displacement of the thiophene ligand in Cp*Ir(η^5-2,5-Me_2T)$^{2+}(I^-)_2$ by the I^- ions would then lead to the product (**11**).

3.4. Reactions of *1* and *2* with maleic anhydride

The reaction of **1** with maleic anhydride in THF solvent over a period of 30 h at room temperature gives (Eq. (12)) two isolated and crystallographically characterized products, **12** and **13**,

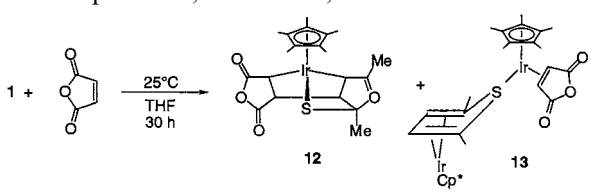

(12)

in 20% and 15% yield, respectively. The most easily rationalized product **13** results from the replacement of the η^4-2,5-Me_2T ligand in one molecule of **1** by another molecule of **1** and a maleic anhydride ligand. The presence of the S-bonded Cp*Ir(η^4-2,5-Me_2T) ligand

illustrates again the strong co-ordinating ability of the sulfur in **1**, as noted in the discussion of Eq. (2).

Complex **2** also reacts with maleic anhydride but gives only product **12** (in 42% yield). The lower reaction temperature (− 40 to − 20°C) and higher yield of **12** suggests that the formation of **12** in Eq. (12) may involve initial isomerization of **1** to **2**, which then reacts with maleic anhydride to give **12**.

The composition and structure of **13** shown in Eq. (12) are supported by elemental analyses as well as mass and ^{1}H-NMR spectra. The structure (Fig. 3) of **13** is related to that of Cp'Rh[η^1(S)–Cp'Rh(η^4-Me_4T)]$_2$, where Cp' = η^5-C_5Me_4Et, which contains two S-bonded Cp'Rh(η^4-Me_4T) ligands [20]. The plane of the η^2-coordinated maleic anhydride ligand in **13** is nearly parallel (14° angle) to the plane of the Cp* ligand on Ir(2).

The structure of product **12** is more complex and is composed of one Cp*Ir(2,5-Me_2T) unit, a maleic anhydride molecule and an oxygen atom. The source of the oxygen atom is not obvious, although the THF solvent and adventitious O_2 are possibilities. Previously [8] we observed that O_2 reacts with **1** and **2** at room temperature over a period of 12–24 h to give (Eq. (13)) the acylthiolate complex Cp*Ir(η^4-SC_3H_2MeC(=O)Me) (**14**). We also observed [21]

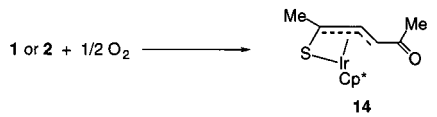

14 (13)

the formation of **14** in reactions of $Re_2(CO)_{10}$ with **1** in THF. Although the source of the oxygen atom in complex **12** is not clear, it seemed possible that the acylthiolate **14** was formed as an intermediate that reacted with maleic anhydride to give the final product **12**. Indeed, **14** reacts with maleic anhydride in THF even at lower temperatures (− 40° to 20°C) during a 24 h period to give **12** in quite high (75%) yield. Thus, **14** is a likely intermediate in the formation of **12** in Eq. (12); a possible mechanism for this conversion is shown in Scheme 1. While this mechanism does account for the atom connectivity in **12**, there is no direct evidence to support it, and one can imagine other possible mechanisms. The formation of **12** again emphasizes the remarkable array of reactions that **1** and **2** undergo [4].

The ^{1}H-NMR spectrum of **12** shows two singlets at δ 2.10 and 1.94 ppm for the non-equivalent methyl groups at C(3) and C(5) in Fig. 2. The four non-equivalent C–H hydrogens at C(1), C(6), C(7), and C(8) each occur as doublets, as expected, at δ 3.95, 3.64, 3.50, and 3.02 ppm. In the structure (Fig. 2) of **12**, all of the C–C single and C(sp^2)=O double bond distances are normal [22] except those associated with the original acyl group. Although the acyl carbonyl bond is represented in the drawings of **12** in Eq. (12) and Scheme 1 as a double bond (in order to make the connectivity easier to visualize), the C(2)–O(1) distance (1.332(7) Å) is very similar to that (1.34 Å) [22] of a normal C(sp^2)–O single bond and is significantly longer than a C(sp^2)=O double bond (1.20 Å), as observed in the anhydride carbonyl groups (C(10)=O(4), 1.205(8); C(9)=O(2), 1.185(7) Å). Thus, C(2)–O(1) appears to be largely a single bond. The C(4)–O(1) bond (1.479(7) Å) is long compared to a normal C(sp^3)–O single bond (1.41 Å), suggesting a weakened interaction here.

The acyl carbon C(2) is planar, as indicated by the sum (359.6°) of the three angles around it. As noted above, the C(2)–O(1) bond is largely a single bond; the C(2)–C(3) bond distance (1.478(9) Å) is also a single bond as compared with a normal C(sp^2)–C(sp^3) distance (1.50 Å). However, the C(1)–C(2) distance (1.404(9)) is short compared to a normal C(sp^3)–C(sp^2) bond (1.50 Å), but is not as short as a C(sp^2)=C(sp^2) double bond (1.34 Å), suggesting some double bond (or strong σ-bond) character between C(1) and C(2). As C(1) is bonded to 4 atoms, this is surprising. Perhaps the short C(1)–C(2) is related to the distorted geometry around C(1) for which the sum of the Ir–C(1)–C(6), Ir–C(1)–C(2), and C(2)–C(1)–C(6) angles is only 300.7° as compared with a normal tetrahedral carbon where this sum would be 328°. The sum of the angles around the other Ir-bonded carbon C(8) is a more normal 329°. Considering the unusual structural features of the 'acyl group' in **12**, it is not clear why the reaction of **14** with maleic anhydride leads to this surprising product.

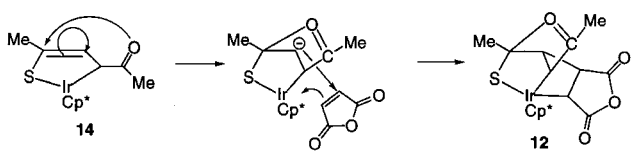

Scheme 1.

4. Supplementary material

Crystallographic data for the structural analyses have been deposited with the Cambridge Crystallographic Data Centre, CCDC Nos 149325, 149326, and 149327 for compounds **3**, **12**, and **13**. Copies of these data may be obtained free of charge from The Director, CCDC, 12 Union Road, Cambridge CB2 1EZ, UK (Fax: + 44-1223-336033; E-mail: deposit@ccdc.cam.ac.uk or www.ccdc.cam.ac.uk

Acknowledgements

The authors thank the US Department of Energy, Office of Science, Office of Basic Energy Sciences, Chemical Sciences Division, under contract W-7405-Eng-82 with Iowa State University. We also thank the

crystallographers: Dr. L.M. Daniels (Texas A&M University) for **3**, Dr. Victor G. Young Jr, (University of Minnesota) for **12**, and Mr Jie Su (Shanghai Institute of Organic Chemistry) for **13**.

References

[1] J. Chen, L.M. Daniels, R.J. Angelici, J. Am. Chem. Soc. 112 (1990) 199.
[2] J. Chen, R.J. Angelici, Organometallics 8 (1989) 2277.
[3] J. Chen, R.J. Angelici, Appl. Organomet. Chem. 6 (1992) 479.
[4] J. Chen, R.J. Angelici, Coord. Chem. Rev. 206–207 (2000) 63.
[5] J. Chen, L.M. Daniels, R.J. Angelici, Polyhedron 9 (1990) 1883.
[6] J. Chen, R.J. Angelici, Organometallics 11 (1992) 992.
[7] J. Chen, R.J. Angelici, Organometallics 9 (1990) 849.
[8] J. Chen, R.J. Angelici, Inorg. Chim. Acta 235 (1995) 61.
[9] L.N. Mander, S.P. Sethi, Tetrahedron Lett. 24 (1983) 5425.
[10] S.H. Smallcombe, H.C. Caserio, J. Am. Chem. Soc. 93 (1971) 5826.
[11] SHELXS-86, G.M. Sheldrick, Institut für Anorganische Chemie der Universität, Göttingen, Germany.
[12] SHELXTL-Plus, Siemens Analytical X-ray, Inc., Madison WI, USA.
[13] B. Bak, D. Christensen, J. Rastrup-Andersen, E. Tannenbaum, J. Chem. Phys. 25 (1956) 892.
[14] M.D. Fryzuk, X. Gao, K. Joshi, P.A. MacNeil, R.L. Massey, J. Am. Chem. Soc. 115 (1993) 10581.
[15] S. Luo, T.B. Rauchfuss, S.R. Wilson, J. Am. Chem. Soc. 114 (1992) 8515.
[16] S. Luo, T.B. Rauchfuss, Z. Gau, J. Am. Chem. Soc. 115 (1993) 4943.
[17] J.W. Hachgenei, R.J. Angelici, J. Organomet. Chem. 355 (1988) 359.
[18] G.H. Spies, R.J. Angelici, Organometallics 6 (1987) 1897.
[19] (a) A. Millan, P.M. Bailey, P.M. Maitlis, J. Chem. Soc. Dalton Trans. (1982) 73. (b) M.R. Churchill, S.A. Julis, Inorg. Chem. 18 (1979) 1215.
[20] S. Luo, A.E. Skaugset, T.B. Rauchfuss, S.R. Wilson, J. Am. Chem. Soc. 114 (1992) 1732.
[21] J. Chen, Jr., V.G. Young, R.J. Angelici, Organometallics 15 (1996) 2727.
[22] J. March, Advanced Organic Chemistry, third ed., Wiley, New York, 1985, p. 19.